CHARMLESS HADRONIC TWO-BODY $B_{\rm s}$ DECAYS WITHIN THE VECTOR QUARK MODEL

M.R. Ahmady

Physics Department, Mount Allison University
New Brunswick, Canada E4L 1E6

F. Falahati, S.M. Zebarjad[†]

Physics Department, Shiraz University, Shiraz 71454, Iran

(Received June 3, 2009)

Charmless two-body decays of $B_{\rm s}$ mesons to PP, PV and VV final states are investigated within an extension of the standard model with an additional vector quark. Besides the CP averaged branching ratio, we look into the direct CP violation associated with each mode to search for those decays which are most sensitive to this new physics scenario. Our results indicate that the branching ratio of $B_{\rm s} \to \pi^0\eta, \pi^0\eta', \pi^0\phi$ receive the most significant shifts from the presence of a singlet quark. On the other hand, the direct CP violations in $B_{\rm s} \to \phi\eta', \phi\phi$ are the most affected by the vector quark model.

PACS numbers: 12.15.Mm, 13.25.Hw, 11.30.Hv

1. Introduction

The Large Hadron Collider (LHC) is expected to expand our experimental reach in b-physics area with the production of a large number of various mesons and baryons containing this quark. Among these, $B_{\rm s}$ meson plays a crucial role in our precision test of the Standard Model (SM) and understanding of the new physics beyond it. For example, some of the charmless decays of $B_{\rm s}$ could be quite sensitive to the presence of any flavor changing neutral current (FCNC) at the tree level which is forbidden within the SM and therefore, could provide excellent testing grounds for some new physics models.

A simple extension of the standard model (SM) is to enlarge the particle content by adding an extra down-type iso-singlet quark, whose right-handed and left-handed components are invariant under the $\mathrm{SU}(2)_{\rm L}\times\mathrm{U}(1)_{\rm Y}$

[†] Corresponding author: `zebarjad@physics.susc.ac.ir`

weak gauge group. This iso-singlet quark which is known as vector down-type quark, can engage in weak interactions only through mixing with ordinary quarks [1, 2]. Consequently, the extended 3×4 quark mixing matrix *is not* unitary, leading to tree-level FCNC. In fact, one can show that in this scenario, which we call Vector Down-type Quark Model or VDQM for abbreviation, tree-level $b \to s$ transition is directly proportional to $(V_{\rm KM}^{\dagger} V_{\rm KM})^{sb}$, where $V_{\rm KM}$ is the 3×3 Kobayashi–Maskawa (KM) quark mixing matrix. Reference [2] contains a more extensive discussion of this interesting aspect of the VDQM. The tree-level $b \to s$ process, even though small, could have significant effects on some rare decay branching ratios and CP violation for hadrons containing a b-quark.

Motivated by the above possibility, we are investigating the effect of adding an extra down-type vector quark to the SM on various charmless $B_{\rm s}$ decays to PP, PV and VV final states, where P and V stand for pseudoscalar and vector mesons, respectively. The CP averaged branching ratio and direct CP asymmetry for each decay channel are calculated and compared with the SM predictions thus looking for observables that can impose the most severe constraints on VDQM parameter space.

The charmless hadronic decays of the $B_{\rm s}$ meson are studied within the framework of generalized factorization in which factorization is applied to the tree level matrix elements while the effective Wilson coefficients are μ and renormalization scheme independent, and nonfactorizable effects are parameterized in terms of $N_c^{\rm eff}(V-A)$ and $N_c^{\rm eff}(V+A)$, the effective numbers of colors arising from $(V-A)(V-A)$ and $(V-A)(V+A)$ four-quark operators, respectively [3]. Similar recent applications of generalized factorization method can be found in [4–6]. As usual in the literature, in the first iteration, one does not consider the effect of the weak annihilation and exchange diagrams although they may have significant contributions in some decay channels and so need to be studied in more accurate treatments of the problem.

This paper is organized as follows. In Sec. 2, we first quote the theoretical framework within the SM, the effective Hamiltonian as well as the generalized factorization formula to obtain the hadronic matrix element for the two body $B_{\rm s}$ decays. The effects of a vector like down quark on the effective Hamiltonian and the hadronic matrix element for $B_{\rm s}$ meson decays are investigated in Sec. 3. The last section is devoted to our conclusions and discussions.

2. The hadronic matrix element for two body $B_{\rm s}$ decays in SM

The standard theoretical framework to calculate the inclusive three-body decays $b \to q\bar{q}'q'$ $(q = d, s)$ is based on the effective Hamiltonian [7, 8],

$$\begin{aligned}\mathcal{H}_{\rm eff} &= \frac{G_{\rm F}}{\sqrt{2}}\Bigg[V_{ub}V_{uq}^*(C_1O_1^u + C_2O_2^u) + V_{cb}V_{cq}^*(C_1O_1^c + C_2O_2^c) \\ &\quad - V_{tb}V_{tq}^*\left(\sum_{i=3}^{10} C_iO_i + C_gO_g\right)\Bigg] + \text{h.c.}\,, \qquad (1)\end{aligned}$$

where the quark operator definitions can be found in Ref. [7, 8] and the SM value of the Wilson coefficients are presented in Refs [8, 9].

As mentioned in the introduction, in order to evaluate the hadronic matrix elements for two body $B_{\rm s}$ decays, $\langle\mathcal{H}_{\rm eff}\rangle$, we use the generalized factorization ansatz in which the quantities $C_i^{\rm eff}$ and $N_c^{\rm eff}$ play the basic roles. To obtain the explicit expressions for $C_i^{\rm eff}$ $(i = 1, \cdots, 10)$, the one-loop matrix elements at quark level are written in terms of the tree-level matrix elements of the effective operators in the following form

$$\langle sq'\bar{q}'|\mathcal{H}_{\rm eff}|b\rangle = \sum_{i,j} C_i^{\rm eff}(\mu)\langle sq'\bar{q}'|O_j|b\rangle^{\rm tree}, \qquad (2)$$

and thus the effective Wilson coefficients $C_i^{\rm eff}$ are extracted. In the NDR scheme, this method leads to [7]:

$$\begin{aligned}C_i^{\rm eff} &= \left[1 + \frac{\alpha_{\rm s}}{4\pi}\left(r_V^{\rm T} + \gamma_V^{\rm T}\log\frac{m_b}{\mu}\right)\right]_{ij} C_j \\ &\quad + \frac{\alpha_{\rm s}}{24\pi}\,A_i'\,(C_t + C_p + C_g)\,, \qquad i = 1\ldots 6\,, \\ C_i^{\rm eff} &= C_i + \frac{\alpha_{\rm ew}}{8\pi}C_e\,, \qquad i = 7, 9\,, \\ C_i^{\rm eff} &= C_i\,, \qquad i = 8, 10\,. \qquad (3)\end{aligned}$$

Here, $A_i' = (0, 0, -1, 3, -1, 3)^{\rm T}$ and the matrices r_V and γ_V as well as the quantities C_t, C_p, and C_g are given in [7, 10].

After obtaining the effective Wilson coefficients at quark level, we sandwich Eq. (2) between the initial and final mesons to obtain the hadronic matrix elements of the type $\langle M_1M_2|O_i|B_{\rm s}\rangle$ where M_1 and M_2 refer to the final mesons. In order to calculate these matrix elements, we split them into a product of two matrix elements of the generic type $\langle M_1|\bar{q}b|B_{\rm s}\rangle$ and $\langle M_2|\bar{q}'q'|0\rangle$, where a Fierz transformation is used so that the flavor quantum numbers of the quark currents match those of the hadrons [7]. Using this

Fierz transformation and the identity $T^a_{\alpha\beta}T^b_{\rho\delta} = -(1/2N_c)\delta_{\alpha\beta}\delta_{\rho\delta} + \frac{1}{2}\delta_{\alpha\delta}\delta_{\beta\rho}$ yield operators which are in the color singlet–singlet and octet–octet forms. This procedure finally leads to the appearing of the effective Wilson coefficients $C_i^{\rm eff}$ in the hadronic matrix elements as the following combinations [7]:

$$a_{2i-1} \equiv C_{2i-1}^{\rm eff} + \frac{C_{2i}^{\rm eff}}{N_c^{\rm eff}}\,, \qquad a_{2i} \equiv C_{2i}^{\rm eff} + \frac{C_{2i-1}^{\rm eff}}{N_c^{\rm eff}}\,, \qquad (i=1,\ldots,5)\,, \tag{4}$$

where $N_c^{\rm eff}$ is the effective number of colors in which the nonfactorizable effects due to the octet–octet and singlet–singlet operators are included. As discussed in Ref. [3], these nonfactorizable effects in the matrix elements of $(V-A)(V-A)$ operators are not the same as those of $(V-A)(V+A)$ operators; $N_c^{\rm eff}(V-A) \neq N_c^{\rm eff}(V+A)$. The analysis of data for B decays in that article shows that the suitable choice for $N_c^{\rm eff}$ is $N_c^{\rm eff}(V-A) < 3 < N_c^{\rm eff}(V+A)$. In the forthcoming numerical analysis, we choose the value of $N_c^{\rm eff}(V-A) = 2$, $N_c^{\rm eff}(V+A) = 5$ which satisfy the above condition, and consistent with values taken for this parameter in the literature [5, 6]. The matrix elements $\langle M_2|\bar{q}'q'|0\rangle$ and $\langle M_1|\bar{q}b|B_{\rm s}\rangle$,which are color singlet, are parameterized in terms of the decay constants and form factors, respectively. The explicit expressions for them can be found in [3, 7].

For the k^2 dependence of the form factors we have chosen the predictions of BSW model [11–13] and our numerical inputs for the decay constants and other parameters are the same as in [10].

Using the described methods, one is able to obtain the decay amplitude for two-body $B_{\rm s}$ decays. These amplitudes are given in Ref. [11], from which one can compute the branching ratios and the direct CP asymmetries for the two body $B_{\rm s}$ decays. Based on the above explanations, we can now investigate the effect of an extra down-type vector quark on these physical quantities.

3. Vector-like Down-Quark Model (VDQM)

We now consider the effect of extending the SM with the addition of an extra down-type iso-singlet quark D. One can show that the 3×4 quark mixing matrix now is bound to be non-unitary and consequently, there are tree-level FCNC proportional to the deviation from unitarity. For example, the $b \to q$ $(q = d, s)$ FCNC is parameterized by a complex parameter $U^{q\,b} = (V^\dagger V)^{q\,b}$ which can enter the Wilson coefficients of the operators in the effective Hamiltonian, Eq. (1). Hence, one can show that the Wilson coefficients C_3, C_7, C_9 and C_g receive the additional contributions due to the FCNC (for the first three ones) and the nonunitarity of CKM matrix (for the last one) at scale $\mu = M_{\rm W}$ as the following [1]:

$$\begin{aligned}
C_3^{\rm VQM} &= U^{q\,b}\tfrac{1}{6}\,, \\
C_7^{\rm VQM} &= U^{q\,b}\tfrac{2}{3}\sin^2\theta_{\rm W}\,, \\
C_9^{\rm VQM} &= -U^{q\,b}\tfrac{2}{3}(1-\sin^2\theta_{\rm W})\,, \\
C_g^{\rm VQM} &= -U^{q\,b}\tfrac{1}{3}\,.
\end{aligned} \tag{5}$$

Using the renormalization group evolution, we can run the $C_i^{\rm VQM}$ from the $M_{\rm W}$ scale to the scale of m_b. For $C_1^{\rm VQM}-C_{10}^{\rm VQM}$, the NLO corrections should be included. While for $C_g^{\rm VQM}$, LO results is sufficient. The details for the running Wilson coefficients can be found in Refs [8, 9]. Based on the above explanations, we can write the new effective Hamiltonian as:

$$\begin{aligned}
\mathcal{H}_{\rm eff} &= \frac{G_{\rm F}}{\sqrt{2}}\Bigg[V_{ub}V_{uq}^*(C_1O_1^u+C_2O_2^u)+V_{cb}V_{cq}^*(C_1O_1^c+C_2O_2^c) \\
&\quad - V_{tb}V_{tq}^*\left(\sum_{i=3}^{10}C_i^{\rm new}O_i+C_g^{\rm new}O_g\right)\Bigg]+{\rm h.c.}\,,
\end{aligned} \tag{6}$$

where $C_i^{\rm new}$ and $C_g^{\rm new}$ are:

$$C_i^{\rm new}=C_i-\frac{C_i^{\rm VQM}}{V_{tb}V_{tq}^*}\,,\qquad i=3\ldots10,g\,. \tag{7}$$

Now, by substituting $C_i \to C_i^{\rm new}$ (for $i=3\ldots10,g$) in Eq. (3), the new effective Wilson coefficients $C_i^{\rm eff\ new}$ can be obtained leading to the $a_i^{\rm new}$ by the replacement of $C_i^{\rm eff}$ with $C_i^{\rm eff\ new}$ in Eq. (4). As a result, we can easily obtain the branching ratios and the direct CP asymmetries for the two body $B_{\rm s}$ decays by substituting $a_i \to a_i^{\rm new}$in all decay amplitudes.

In the next section, by considering the constraint on the vector quark model parameters, we analyze the effect of this new quark on the branching ratio and the direct CP asymmetries of the hadronic $B_{\rm s}$ decays.

4. Numerical results and their analysis

The most recent experimental data from Belle [17] and BABAR [18] on the branching ratio of the inclusive $B_{\rm s}\to X_{\rm s}\ell^+\ell^-$ decay impose sever constraints on the phase and magnitude of U^{sb} which is shown in Fig. 1 [14]. The range of ϕ^{sb} is indeed between 0 and 2π which can be obtained by reflecting the $0<\phi^{sb}<\pi$ region with respect to $|U^{sb}|$ axis on the top. In the present section, we use this restriction on U^{sb} to analyze numerically the

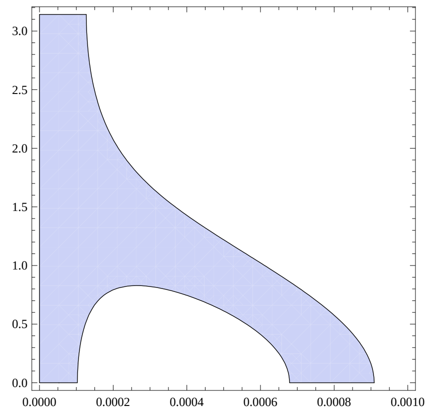

Fig. 1. The allowed region of VDQM parameters, $|U^{sb}|$ and ϕ^{sb}, obtained by considering the most recent experimental data on the branching ratio of the inclusive $B_{\rm s} \to X_{\rm s}\ell^+\ell^-$ decay.

effect of an extra down-type vector quark on the branching ratios and the direct CP asymmetries for the two body $B_{\rm s}$ decays. Moreover, we ignore the decays involving $b \to d$ transition since U^{db} is expected to be an order (orders) of magnitude smaller than U^{sb}. As for the CKM matrix elements, we shall use the Wolfenstein parametrization [15] with the following parameter values [16]: $A = 0.8533 \pm 0.0512$, $\lambda = 0.2200 \pm 0.0026$, $\bar{\rho} = 0.20 \pm 0.09$, and $\bar{\eta} = 0.33 \pm 0.05$. The CP averaged branching ratios within the SM and VDQM for those values of $|U^{sb}|$ and ϕ^{sb} which produce the maximum shift within the allowed domain of these parameters are presented in Tables I–III for PV, VV and PP final states, respectively. Furthermore, the direct CP asymmetry for the above modes are given in Tables IV–VI. From these tables, we can see the effect of VDQM to the branching ratios and CP violation is both constructive and destructive in the allowed region of Fig. 1. In addition, this new physics scenario may flip the sign of the direct CP violation. The detailed discussion of these behaviors are presented in the following:

- **Table I:** The $B_{\rm s} \to \phi\pi$ decay is the most sensitive process among the $B_{\rm s} \to PV$ decays to the new physics. The branching ratio of this decay changes almost from $1/2$ to 9 times of that of the SM (Fig. 2). The sensitivity of $B_{\rm s} \to \rho\eta$ and $B_{\rm s} \to \rho\eta'$ to the VDQM parameters are the same with the enhancement of the branching ratio up to 4 times of the SM value which is more significant than the maximum possible reduction of about 29% of the SM prediction. In both $B_{\rm s} \to \omega(\eta, \eta')$ decays, the minimum values of branching ratio are $1/3$ of those of the SM and the maximum boost amounts to almost 2 times of those of the SM.

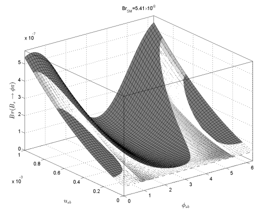

Fig. 2. The plot of the branching ratio in $B_{\rm s} \to \phi\pi$ as a function of the phase ϕ^{sb} and the magnitude of U^{sb}.

The sensitivity of $B_{\rm s} \to \phi\eta$ and $B_{\rm s} \to \phi\eta'$ to the VDQM parameters are not the same. The constructive contribution of new physics in $B_{\rm s} \to \phi\eta$ enhances the magnitude of the SM branching ratio by a factor of 2.5 which is much larger than the destructive one. However, in the $B_{\rm s} \to \phi\eta'$ process, the destructive contribution of VDQM could reduce the magnitude of the branching ratio almost to 1/4 of the SM prediction and is more significant than the constructive one. As for $B_{\rm s} \to \overline{K}^{*0} K^0$, the VDQM can give about 33% enhancement to the branching ratio.

- **Table II:** The $B_{\rm s} \to \rho\phi$ decay is the most sensitive process among the $B_{\rm s} \to VV$ decays to the new physics. The maximum value of branching ratio of this decay is around 4 times of that of the SM (Fig. 3). In $B_{\rm s} \to \omega\phi$ decay, the VDQM model reduces the branching ratio to 1/3 of the SM value and increases it to 2 times of what is expected from the SM. On the other hand, the destructive contribution to $B_{\rm s} \to \phi\phi$ decay brings down the branching ratio to 1/2 of the SM value.

- **Table III:** $B_{\rm s} \to \pi^0\eta$ and $B_{\rm s} \to \pi^0\eta'$ decays receive the largest enhancements from VDQM with branching ratios going up by a factor 9 compared to that of the SM predictions (Fig. 4). The possible destructive contributions to the branching ratios are more modest reducing it by a factor 1/2. Along with $B_{\rm s} \to \phi\pi$ decay, the above channels are the most promising venues among the charmless two body decays of $B_{\rm s}$ to test the validity of VDQM. Other $B_{\rm s} \to PP$ decays get less sizable shifts in their branching ratios due to the presence of a single down-type vector quark.

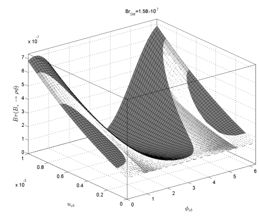

Fig. 3. The plot of the branching ratio in $B_{\rm s} \to \rho\phi$ as a function of the phase ϕ^{sb} and the magnitude of U^{sb}.

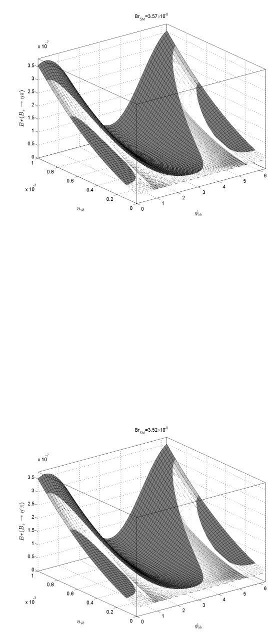

Fig. 4. The plots of the branching ratio in $B_{\rm s} \to \pi\eta$ and $B_{\rm s} \to \pi\eta'$ as functions of the phase ϕ^{sb} and the magnitude of U^{sb}.

- **Table IV:** The direct CP asymmetry in $B_s \to \phi\eta'$ decays can change by more than an order of magnitude as well as receive a sign change due to the presence of the extra quark (Fig. 5). Replacing η' with η in the final state leads to a smaller shift of around a factor 4 in the direct CP violation.

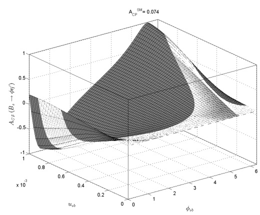

Fig. 5. The plot of the CP asymmetry in $B_s \to \phi\eta'$ as a function of the phase ϕ^{sb} and the magnitude of U^{sb}.

- **Table V:** Among the VV modes of the B_s decays, $B_s \to \phi\phi$ shows the largest sensitivity to VDQM, asymmetries up to 15% (plus or minus sign) are possible as compared to SM prediction of nearly zero asymmetry (Fig. 6).

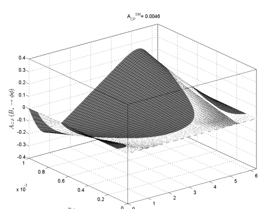

Fig. 6. The plot of the CP asymmetry in $B_s \to \phi\phi$ as a function of the phase ϕ^{sb} and the magnitude of U^{sb}.

- **Table VI:** Our results indicate that the direct CP violation in $B_s \to PP$ modes does not provide an experimentally discern able evidence for the existence of an extra down-type vector quark.

TABLE I

CP averaged branching ratios for charmless $B_s^0 \to PV$ decays in SM and VDQM. The first and second line for each decay mode refer to the minimum and maximum value of the branching ratio in the allowed parameter space of VDQM, respectively.

Decay channel	SM	VLDQ	$\|U^{sb}\|$	ϕ^{sb}
$B_s \to \overline{K}^0 K^{*0}$	3.49×10^{-6}	3.12×10^{-6}	0.00091	0,2π
		3.54×10^{-6}	0.00013	π
$B_s \to \overline{K}^{*0} K^0$	5.92×10^{-7}	5.67×10^{-7}	0.00013	π
		7.89×10^{-7}	0.00091	$0, 2\pi$
$B_s \to K^{*+} K^-$	2.89×10^{-6}	2.79×10^{-6}	0.00026	4.48
		3.38×10^{-6}	0.00088	0.30
$B_s \to K^+ K^{*-}$	1.19×10^{-6}	9.26×10^{-7}	0.00088	5.98
		1.25×10^{-6}	0.00026	1.80
$B_s \to \omega\eta$	1.17×10^{-8}	4.16×10^{-9}	0.00056	1.10
		2.55×10^{-8}	0.00071	5.48
$B_s \to \omega\eta'$	1.15×10^{-8}	4.09×10^{-9}	0.00056	1.10
		2.51×10^{-8}	0.00071	5.48
$B_s \to \phi\eta$	1.82×10^{-7}	1.32×10^{-7}	0.00021	5.48
		4.24×10^{-7}	0.00086	0.40
$B_s \to \phi\eta'$	1.15×10^{-6}	3.25×10^{-7}	0.00091	0.10
		1.39×10^{-6}	0.00013	3.48
$B_s \to \rho\eta$	9.52×10^{-8}	6.72×10^{-8}	0.00017	3.98
		3.77×10^{-7}	0.00091	0.10
$B_s \to \rho\eta'$	9.36×10^{-8}	6.61×10^{-8}	0.00017	3.98
		3.71×10^{-7}	0.00091	0.10
$B_s \to \phi\pi$	5.41×10^{-8}	2.58×10^{-8}	0.00015	3.78
		4.76×10^{-7}	0.00091	0.10

TABLE II

Same as Table I except for $B_s^0 \to VV$.

Decay channel	SM	VLDQ	$\|U^{sb}\|$	ϕ^{sb}
$B_s \to \overline{K}^{*0} K^{*0}$	2.68×10^{-6}	2.40×10^{-6}	0.00091	0,2π
		2.72×10^{-6}	0.00013	π
$B_s \to K^{*+} K^{*-}$	2.48×10^{-6}	2.40×10^{-6}	0.00026	4.48
		2.90×10^{-6}	0.00088	0.30
$B_s \to \omega\phi$	1.94×10^{-8}	6.91×10^{-9}	0.00056	1.10
		4.23×10^{-8}	0.00071	5.48
$B_s \to \phi\phi$	6.19×10^{-6}	3.17×10^{-6}	0.00091	0,2π
		6.71×10^{-6}	0.00013	3.00
$B_s \to \rho\phi$	1.58×10^{-7}	1.11×10^{-7}	0.00017	3.98
		6.25×10^{-7}	0.00091	0.10

TABLE III

Same as Table I except for $B_s^0 \to PP$.

Decay channel	SM	VLDQ	$\|U^{sb}\|$	ϕ^{sb}
$B_s \to \overline{K}^0 K^0$	1.33×10^{-5}	1.32×10^{-5}	0.00091	0,2π
		1.33×10^{-5}	0.00013	π
$B_s \to K^+ K^-$	1.22×10^{-5}	1.21×10^{-5}	0.00015	3.78
		1.27×10^{-5}	0.00091	0.10
$B_s \to \pi^0\eta$	3.57×10^{-8}	1.70×10^{-8}	0.00015	3.78
		3.14×10^{-7}	0.00091	0.10
$B_s \to \pi^0\eta'$	3.52×10^{-8}	1.68×10^{-8}	0.00015	3.78
		3.10×10^{-7}	0.00091	0.10
$B_s \to \eta\eta'$	2.32×10^{-5}	1.87×10^{-5}	0.00091	0,2π
		2.38×10^{-5}	0.00013	3.00
$B_s \to \eta\eta$	7.00×10^{-6}	5.43×10^{-6}	0.00091	0,2π
		7.19×10^{-6}	0.00013	2.90
$B_s \to \eta'\eta'$	1.73×10^{-5}	1.42×10^{-5}	0.00091	0,2π
		1.78×10^{-5}	0.00013	π

TABLE IV

Direct CPV for charmless $B_s^0 \to PV$ decays in SM and VDQM. The first and second line for each decay mode refer to the minimum and maximum value of the direct CP violation in the allowed parameter space of VDQM, respectively.

Decay channel	SM	VLDQ	$\lvert U^{sb}\rvert$	ϕ^{sb}
$B_s \to \overline{K}^0 K^{*0}$	0.0036	−0.013	0.00066	0.90
		0.020	0.00066	5.38
$B_s \to \overline{K}^{*0} K^0$	0.0007	−0.012	0.00061	5.28
		0.014	0.00061	1.00
$B_s \to K^{*+} K^-$	0.28	0.23	0.00086	5.88
		0.29	0.00029	1.70
$B_s \to K^+ K^{*-}$	−0.053	−0.068	0.0009	0.20
		−0.050	0.00029	4.58
$B_s \to \omega\eta$	0.48	0.30	0.00088	5.98
		0.73	0.00051	1.20
$B_s \to \omega\eta'$	0.48	0.30	0.00088	5.98
		0.73	0.00051	1.20
$B_s \to \phi\eta$	−0.26	−1.00	0.00043	0.80
		1.00	0.00056	5.28
$B_s \to \phi\eta'$	0.074	−0.77	0.00079	0.60
		0.90	0.00083	5.78
$B_s \to \rho\eta$	0.046	−0.016	0.00056	5.18
		0.072	0.00021	2.00
$B_s \to \rho\eta'$	0.046	−0.016	0.00056	5.18
		0.072	0.00021	2.00
$B_s \to \phi\pi$	0	0		
		0		

TABLE V

Same as Table IV except for $B_s^0 \to VV$.

Decay channel	SM	VLDQ	$\lvert U^{sb}\rvert$	ϕ^{sb}
$B_s \to \overline{K}^{*0} K^{*0}$	0.0036	−0.013	0.00066	0.90
		0.020	0.00066	5.38
$B_s \to K^{*+} K^{*-}$	0.28	0.23	0.00086	5.88
		0.29	0.00029	1.70
$B_s \to \omega\phi$	0.48	0.30	0.00088	5.98
		0.73	0.00051	1.20
$B_s \to \phi\phi$	0.0046	−0.15	0.00075	0.70
		0.15	0.00075	5.58
$B_s \to \rho\phi$	0.046	−0.016	0.00056	5.18
		0.072	0.00021	2.00

TABLE VI

Same as Table IV except for $B_s^0 \to PP$.

Decay channel	SM	VLDQ	$\lvert U^{sb}\rvert$	ϕ^{sb}
$B_s \to \overline{K}^0 K^0$	0.0028	0.0017	0.00066	5.38
		0.0040	0.00066	0.90
$B_s \to K^+K^-$	0.089	0.080	0.00071	5.48
		0.095	0.00056	1.10
$B_s \to \pi^0\eta$	0	0	—	—
		0	—	—
$B_s \to \pi^0\eta'$	0	0	—	—
		0	—	—
$B_s \to \eta\eta'$	0.0024	−0.029	0.00071	0.80
		0.033	0.00066	5.38
$B_s \to \eta\eta$	0.012	−0.049	0.00071	0.80
		0.020	0.00066	5.38
$B_s \to \eta'\eta'$	−0.013	−0.015	0.00066	0.90
		0.041	0.00071	5.48

5. Conclusions

In this paper, we have investigated various two-body charmless decays of the B_s meson. The presence of an extra down-type vector quark results in some significant shifts in the branching ratio and direct CP asymmetry of a number of these decay channels. With the large number of B_s mesons that are expected to be produced at LHC, these processes should be well within the experimental reach and therefore the current analysis can provide further constraints on the model parameters once the data will become available.

REFERENCES

[1] Chia-Hung V. Chang, Darwin Chang, Wai-Yee Keung, *Phys. Rev.* **D61**, 053007 (2000).

[2] M. Ahmady, M. Nagashima, A. Sugamoto, *Phys. Rev.* **D64**, 054011 (2001) [hep-ph/0105049].

[3] H.Y. Cheng, B. Tseng, *Phys. Rev.* **D58**, 094005 (1998).

[4] S.S. Bao, F. Su, Y.L. Wu, C. Zhuang, *Phys. Rev.* **D77**, 095004 (2008).

[5] Y.L. Wu, C. Zhuang, *Phys. Rev.* **D75**, 115006 (2007).

[6] A.K. Giri, B. Mawlong, R. Mohanta, *Phys. Rev.* **D74**, 114001 (2006).

[7] A. Ali, G. Kramer, C.D. Lü, *Phys. Rev.* **D58**, 094009 (1998).

[8] A.J. Buras, R. Fleischer, in *Heavy Flavor II*, Ed. A.J. Buras and M. Lindner, World Scientific, Singapore 1998, p. 65; A.J. Buras, in *Probing the Standard Model of Particle Interactions*, Ed. F. David and R. Gupta, 1998 Elsevier Science B.V., `hep-ph/9806471`.

[9] G. Buchalla, A.J. Buras, M.E. Lautenbacher, *Rev. Mod. Phys.* **68**, 1125 (1996).

[10] Y.H. Chen, H.Y. Cheng, B. Tseng, K.C. Yang, *Phys. Rev.* **D60**, 094014 (1999).

[11] Y.H. Chen, H.Y. Cheng, B. Tseng, *Phys. Rev.* **D59**, 074003 (1999) `[hep-ph/9809364]`.

[12] M. Wirbel, B. Stech, M. Bauer, *Z. Phys.* **C29**, 637 (1985); M. Bauer, B. Stech, M. Wirbel, *Z. Phys.* **C34**, 103 (1987).

[13] D.S. Du, Z.Z. Xing, *Phys. Rev.* **D48**, 3400 (1993); D.S. Du, M.Z. Yang, *Phys. Lett.* **B358**, 123 (1995).

[14] M.R. Ahmady, F. Mahmoudi, P. deNiverville, in preparation.

[15] L. Wolfenstein, *Phys. Rev. Lett.* **51**, 1945 (1983).

[16] [Particle Data Group] W.M. Yao *et al., J. Phys. G* **33**, 1 (2006).

[17] [BELLE Collaboration] T. Iwasaki *et al., Phys. Rev.* **D72**, 092005 (2005).

[18] [BABAR Collaboration] T. Aubert *et al., Phys. Rev. Lett.* **93**, 081802 (2004).